TEST AND ANALYSIS OF CRACKED LUG

A. F. Liu* and H. P. Kan**

INTRODUCTION

For many years, fatigue has been recognized as a potential threat to the safety and reliability of aircraft, automobile, and machinery components. Recent cases of catastrophic failure on high performance aircraft due to the presence of undetected cracks have focused attention on the use of fracture mechanics as an engineering tool to augment traditional static and fatigue design and qualification requirements. Fatigue performance of the pin loaded lug has been thoroughly studied [1, 2]. However, until the present time, investigators have made very little effort on the fracture mechanis aspects of this class of structural configuration. In this paper, a two dimensional lug configuration, shown in Figure 1, is considered. The lug consists of a circular hole embedded inside the semi-circular head. The loading condition is such that a concentrated force is applied through the pin (filled inside the hole) and uniform stresses are reacted at the other end of the strip. It is assumed that through-the-thickness crack, or cracks are at the edge of the hole in a plane perpendicular to the loading direction. Crack tip stress intensity factor is treated as a function of three dimensionless parameters. These independent variables are: c/r, the crack length to hole radius ratio, W/r, the specimen width to hole radius ratio, and W/L, the width to length ratio. Recently, stress intensity factors for some lugs having specific combinations of c/r and W/r ratios have been determined by using cracked finite element analysis [3, 4]. However, a closed form exact solution is not available. In the theory of linear elastic fracture mechanics, stress intensity solution for a given geometry under complex loading condition can be derived by solving the problem with the use of a superimposed stress function. Engineers have stretched their imagination and applied the superposition principle to estimate approximate K factors for complex configurations and loading conditions by combining an appropriate set of available simple stress intensity solutions [5 - 8]. In this paper, approximate K expressions for pin loaded lugs (Figure 1), with one or two cracks at hole, are developed by compounding known stress intensity solutions. The compounded K factors are conveniently expressed in analytical form. However, to present a list of all the geometry factors involved in the compounded K expressions would be too lengthy and beyond the scope of this paper. Therefore, only the methods of formulations are outlined here. In the second phase of this paper, stress intensity factors for the two cracks at hole configuration will be determined by cracked finite element analyses and comparison of results are presented. In the third phase of this paper, crack growth history predicted by using the compounded K factors is compared with actual cyclic crack growth test results of titanium lugs containing thru-crack at one side of the pin loaded hole.

* Northrop Corporation, Aircraft Division, Hawthorne, California, U. S. A.
** Rockwell International, Space Division, Downey, California, U. S. A.

THE COMPOUNDED STRESS INTENSITY EXPRESSION

Consider a lug subjected to a concentrated force (per unit thickness), P/B, at centre of the pin as shown in Figure 1. The total stress intensity would be the sum of the stress intensity due to the concentrated force, K^{P2}, and the stress intensity due to the reacting stress at the end of the lug, K^{S2}. Here the superscripts P, S, and 2 denote pin load, stress, and two cracks, respectively. The pin load causes the crack to open and slide simultaneously, therefore, the stress intensity expression for the pin load is made up of two parts:

$$K_I^{P2} = \frac{1}{2}\left(\frac{P}{B}\right)\psi^{P2}/\sqrt{\pi a} \tag{1}$$

and

$$K_{II}^{P2} = \frac{1}{2}\left(\frac{\chi-1}{\chi+1}\right)\left(\frac{P}{B}\right)\psi^{P2}/\sqrt{\pi a} \tag{2}$$

where a is the equivalent half crack length, equal to (r+c). ψ^{P2} is the geometry factor associated with the pin load. For plane stress condition $\chi = (3-\nu)/(1+\nu)$. Applying the maximum tensile stress criterion, the resultant stress intensity due to the pin load can be expressed as

$$K^{P2} = \sqrt{(K_I^{P2})^2 + (K_{II}^{P2})^2} \tag{3}$$

Since the reacting stress, S, only induces Mode I crack tip stress singularity, the second term of the K factor can be simple expressed as

$$K^{S2} = \frac{1}{2}\left(\frac{P}{WB}\right)\psi^{S2}\sqrt{\pi c} \tag{4}$$

where ψ^{S2} is the geometry factor associated with the reacting stress. The geometry factors in the above equations can be constructed by combining existing stress intensity solutions for circular plate and square plate under specific loading conditions. These geometry factors are available in [9].

If crack is on only one side of the hole, simply modify equations (1) - (4) as follows:

$$K_I^{P1} = \frac{1}{2}\left(\frac{P}{B}\right)\psi^{P1}\sqrt{\frac{a-e}{a+e}}\ /\sqrt{\pi a} \tag{1a}$$

$$K_{II}^{P1} = \frac{1}{2}\left(\frac{\chi-1}{\chi+1}\right)\left(\frac{P}{B}\right)\psi^{P1}\sqrt{\frac{a-e}{a+e}}\ /\sqrt{\pi a} \tag{2a}$$

$$K^{P1} = \sqrt{(K_I^{P1})^2 + (K_{II}^{P1})^2} \tag{3a}$$

$$K^{S1} = \frac{1}{2}\left(\frac{P}{WB}\right)\psi^{S1}\sqrt{\pi c} \tag{4a}$$

with e = c/2 and a = (2r+c)/2. Figures 2a and 2b show the normalized stress intensity factors F^1 (for one crack) and F^2 (for two cracks) as functions of c/r and r/W. Here

$$F^i = \left(K^{Pi} + K^{Si}\right)\left(\frac{WB}{P}\right)/\sqrt{\pi c} \tag{5}$$

with i being equal to 1 or 2, whichever case is appropriate. Note that in these figures, the effect of length is eliminated by assuming that the specimen length is greater than twice the width of the specimen.

THE FINITE ELEMENT MODEL

The lug finite element model, shown in Figure 1, was constructed by using a combination of the singular cracked finite element and other conventional membrane elements. The singular cracked finite element used in this study was the so-called "Hybrid" element. This special element was originally developed by Pian et al, [10], and subsequently modified by Chu [11]. As shown in Figure 3, the system uses four rectangular shaped special elements at each crack tip and each element consists of four nodal points. This finite element formulation calculates stress intensity values for Mode I and Mode II, separately. However, the K_I term is a lumped sum of stress intensities coming from both the pin load and the reacting stress. The K_{II} term is a function of the pin load only. As equations (3) and (5) indicate, the pin load part of K_I interacts with K_{II}; and the total stress intensity factor equals the reacting stress part of K_I plus the vector sum of the K factors for the pin load. Examining equations (1) and (2), one may observe the K_{II}^P is numerically related to K_I^P by a physical constant, i.e.,

$$K_{II}^P = \eta \cdot K_I^P$$

with $\eta = (\chi-1)/(\chi+1)$. Using this relationship, and equation (3), we have

$$F^f = \left\{K_I^f + \left(\sqrt{1+\frac{1}{\eta^2}} - \frac{1}{\eta}\right)K_{II}^f\right\}\left(\frac{WB}{P}\right)\ /\sqrt{\pi c} \tag{6}$$

Here the superscript f indicates that the K values in equation (6) are calculated by finite element modelling. The F factors in equations (5) and (6) are directly comparable.

So far, finite element analysis has been completed for the two-crack configuration with r/W = 0.125. The results are plotted in Figure 2b and show that numerical values agree with the compounded SIF's. Note, in the finite element model, a bearing pressure distribution of the form $p = 2P \cdot \cos\theta/\pi rB$ has been assumed to simulate the actual loading conditions (see Figure 3b). Figure 3c also shows another type of load distribution, $p = 3P \cdot \cos^2\theta/4rB$, which can possibly be close to the actual loading condition. The concentrated force condition shown in Figure 3a is the ideal case and also is being considered in this study. Results from finite element analysis indicate that using cosine square distribution would yield a 4% higher stress intensity factor and the concentrated force condition gives a 7% higher stress intensity factor as compared to those obtained from the cosine distribution.

TEST AND CORRELATIONS

Five specimens were fabricated from two different heats of Ti, 6Al-4V, in annealed condition. The specimen geometries were those shown in Figure 1

but having only one crack at the edge of the hole. The specimens were 25.4 centimeters long and .635 centimeter thick. The hole diameter was either 2.54 or 5.08 centimeters and the specimen width was either 7.62 or 10.16 centimeters. Constant amplitude cyclic load tests were conducted using an MTS 2 MN dynamic frame at target load levels of 67,000 N, maximum, and 6,700 N, minimum. Crack length versus cycles records were determined by using a thermal colouring procedure as follows: First the specimen was machined with an elox cut of approximately 0.05 centimeter at the edge of the hole. After the specimen had been cycled for a certain number of cycles, the specimen was baked in an oven at 510°C for 45 minutes. The specimen was subjected to cyclic loading again for certain number of cycles and then the specimen was returned to the oven for another 45 minutes at the same temperature. Whenever possible, this routine was repeated four times to produce four colour marking bands representative of four crack length increments. Following the last heat tint cycle, cyclic load testing was continued until the crack was advanced close to the edge of the specimen. Finally, the specimen was pulled to failure.

Data correlations were accomplished by comparing the predicted crack growth history with test results. To do this, the first coloured heat band in each specimen was used as the initial crack length in order to eliminate scatters attributed to initiation of fatigue crack from the elox cut. The compounded stress intensity factors were used in association with the material baseline dc/dN curves generated from testing of compact specimens per ASTM standard procedure. The CT specimens data are presented in Figure 4 and the comparisons between the titanium lug tests and predictions are presented in Figure 5. Note that the calculations shown in Figure 5 were based on the apparent upper and lower bound dc/dN properties as indicated in Figure 4. Also, note that during the later stage of the Lug No. 4 test, a second crack (corner crack) was developed at the opposite edge of the hole. The appearance of this second crack might have caused a higher stress intensity factor and consequently higher growth rate of the major crack. In general, all the data correlated well as predicted.

REFERENCES

1. SCHIJVE, J., "Contributions to the Theory of Aircraft Structures", Nijgh-Wolters Noordhoff University Press, 1972, 423.
2. HEYWOOD, R. B., "Designing Against Fatigue of Metals", Reinhold Pub. Corp., New York, New York, 1962.
3. ABERSON, J. A. and ANDERSON, J. M., NASA TMS 2893, 1974, 531.
4. ORRINGER, O., AFFDL-TR-75-51, 1976.
5. BRUSSAT, T. R. and CHIU, S. T., Report No. LR27431, Lockheed-California Co., Burbank, California, 1975.
6. CARTWRIGHT, D. J. and ROOKE, D. P., Engineering Fracture Mechanics, 6, 1974, 563.
7. LIU, A. F., Engineering Fracture Mechanics, 4, 1972, 175.
8. BROEK, D., "Elementary Engineering Fracture Mechanics", Noordhoff International Publishing, Leyden, The Netherlands, 1974.
9. TADA, H., PARIS, P. C. and IRWIN, G. R., "The Stress Analysis of Cracks Handbook", Del Research Corp., Hellertown, Pennsylvania, 1973.
10. PIAN, T. H. H., TONG, P. and LUK, C. H., Third Conference on Matrix Methods in Structural Mechanics, Wright-Patterson AFB, 1971.
11. CHU, K. S., Eighth National Symposium on Fracture Mechanics, Brown University, 1974.

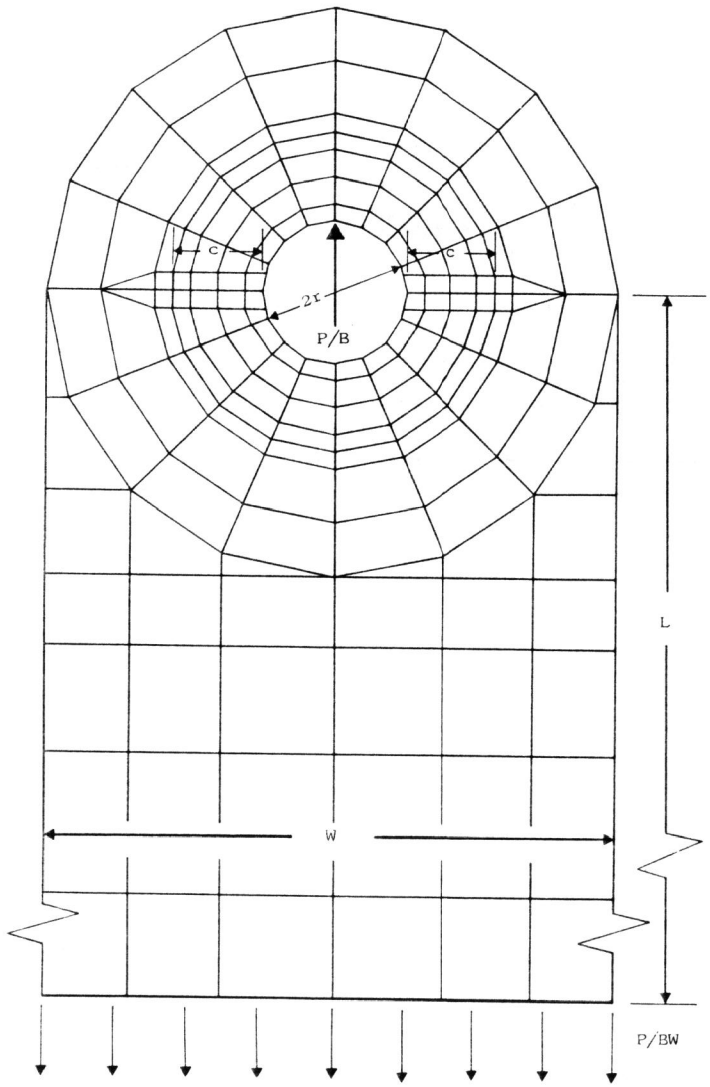

Figure 1 Finite Element Model of Lug Configuration with Two Cracks

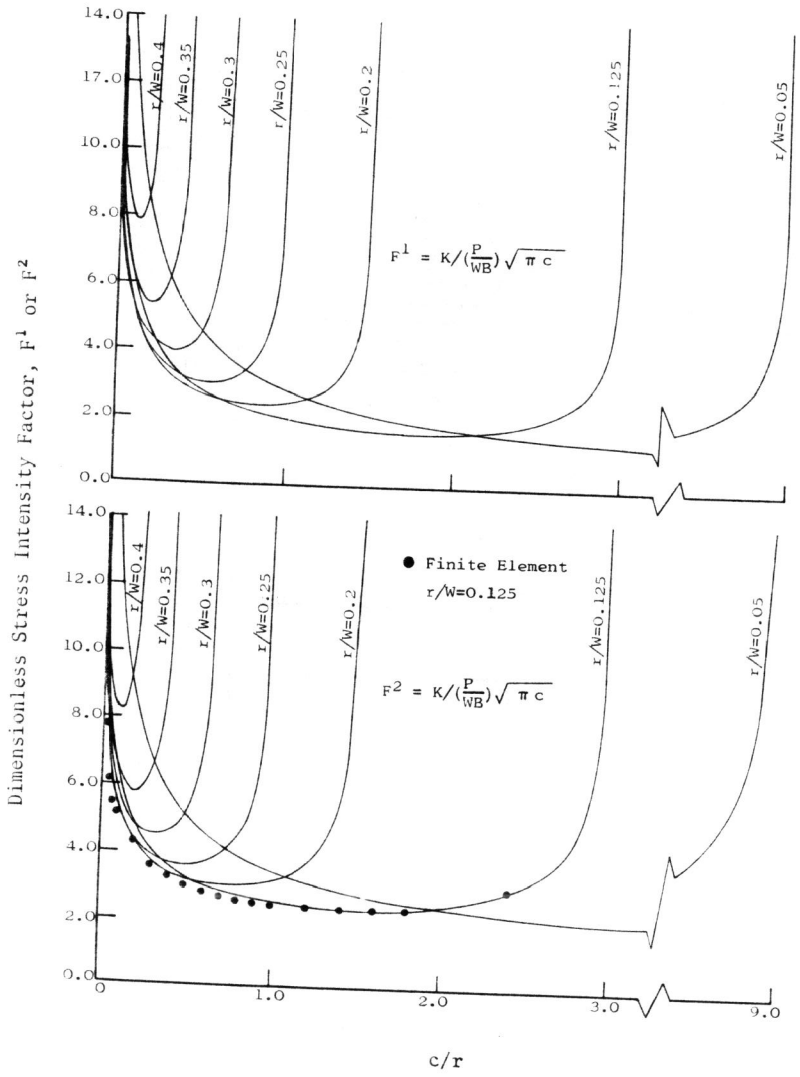

Figure 2 Dimensionless Stress Intensity Factor

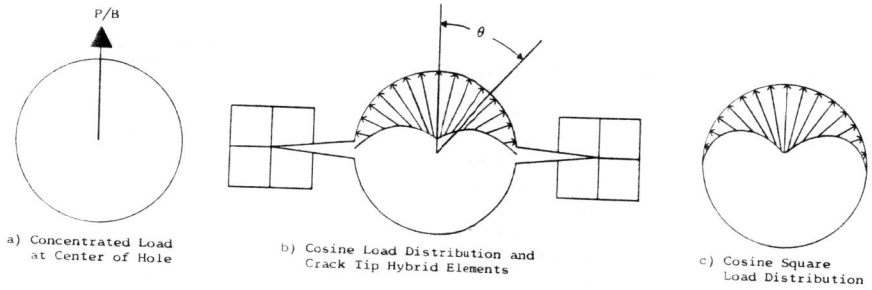

Figure 3 Assumed Load Distribution and Crack Tip Elements

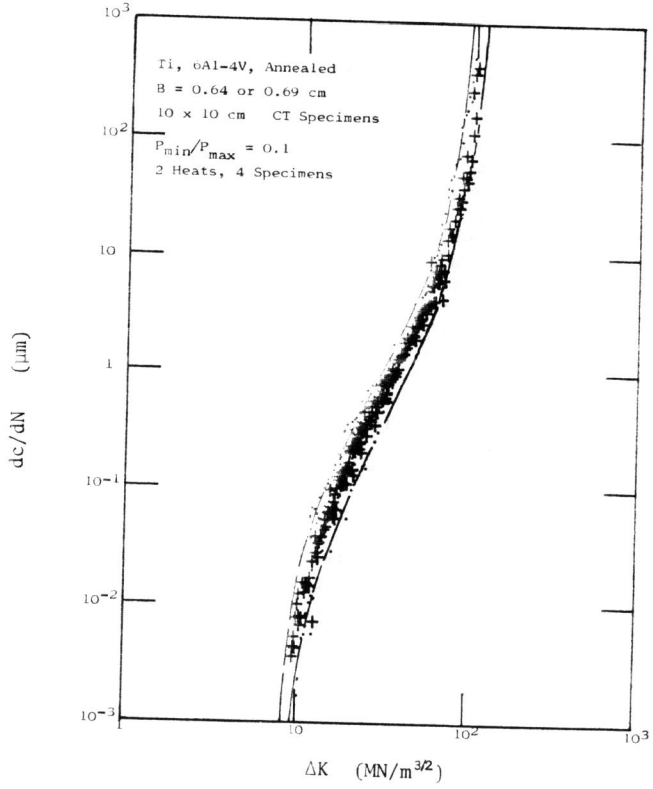

Figure 4 Baseline Crack Growth Rate Data

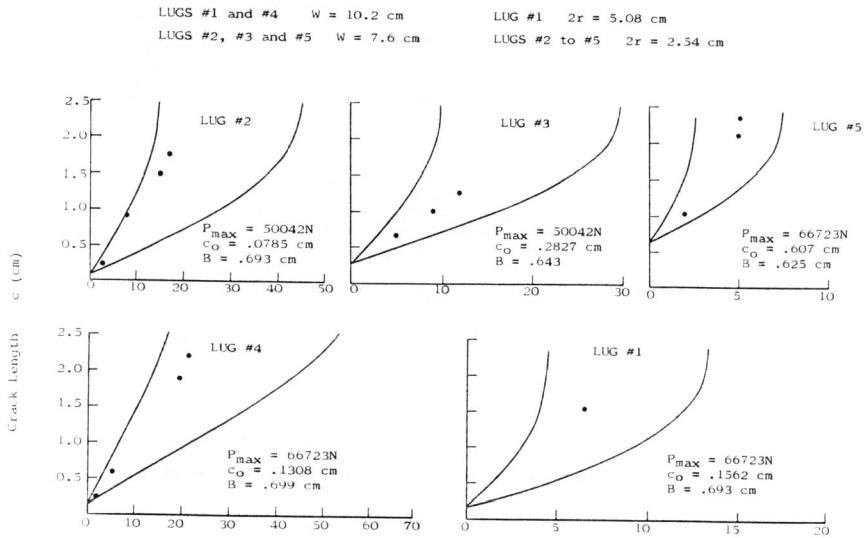

Figure 5 Comparison of Predictions and Test Results